

Molecular Cell, Volume 53

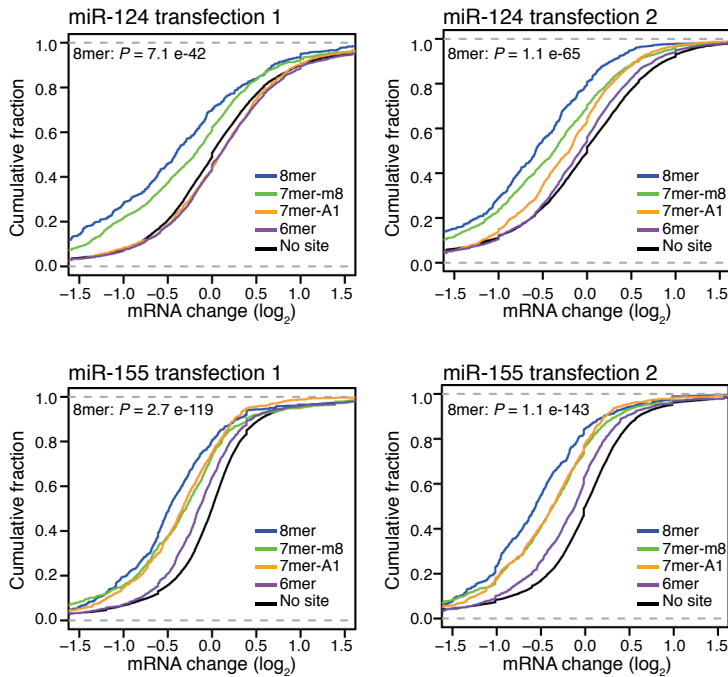
Supplemental Information

Global Analyses of the Effect of Different Cellular Contexts on MicroRNA Targeting

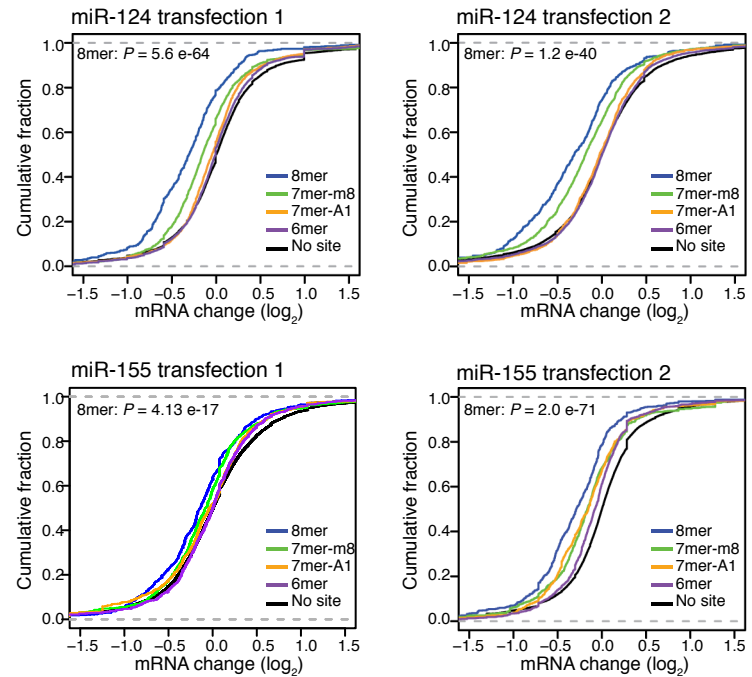
Jin-Wu Nam, Olivia S. Rissland, David Koppstein, Cei Abreu-Goodger, Calvin H. Jan, Vikram Agarwal,
Muhammed A. Yildirim, Antony Rodriguez, and David P. Bartel

A

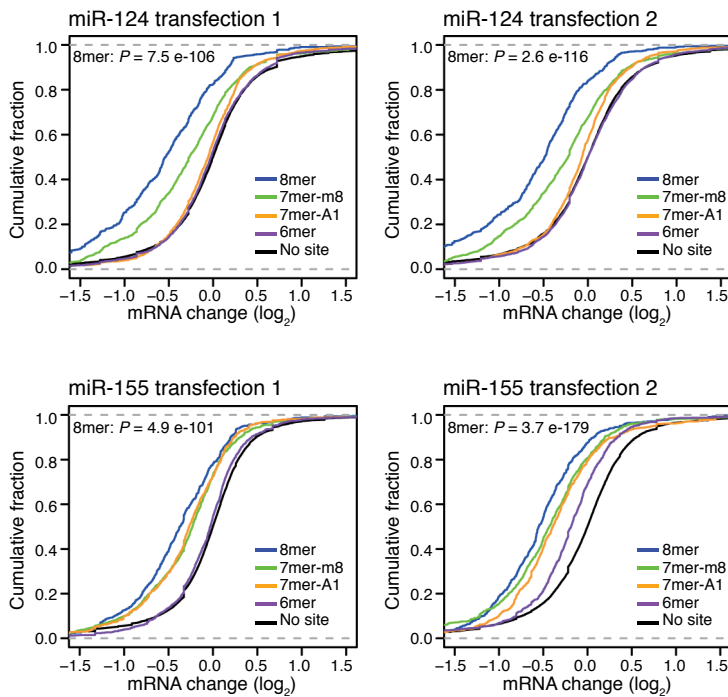
HeLa transfections



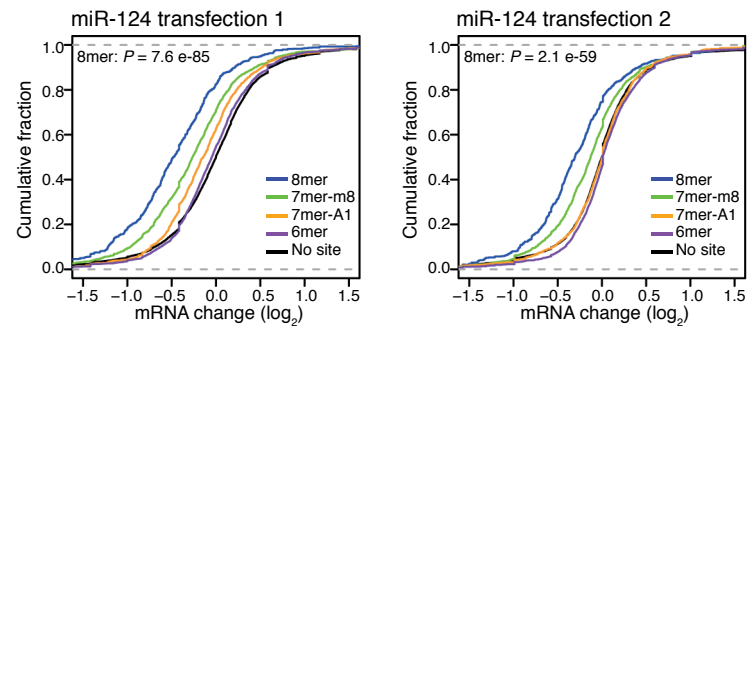
Huh7 transfections



HEK293 transfections

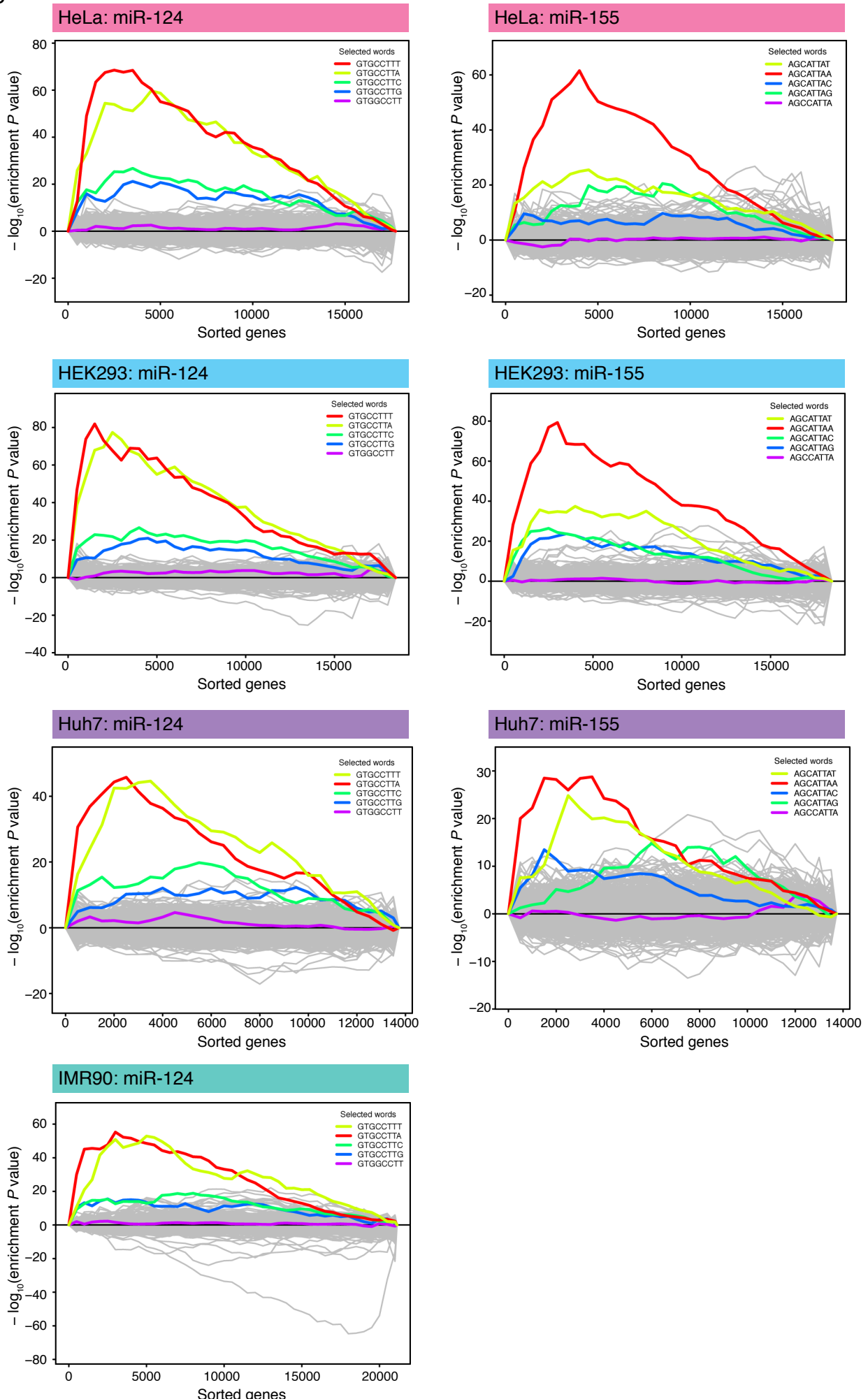


IMR90 transfections



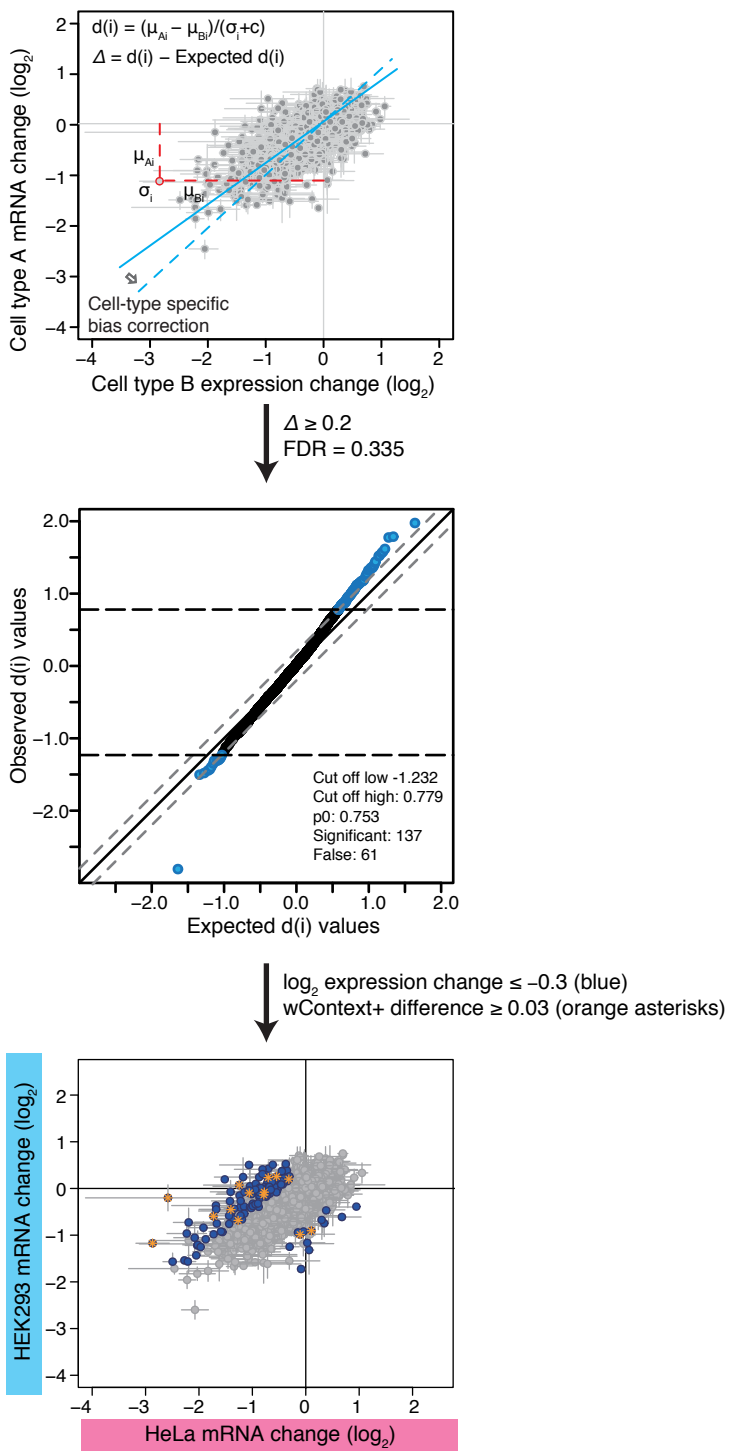
Supplemental Figure 1

B



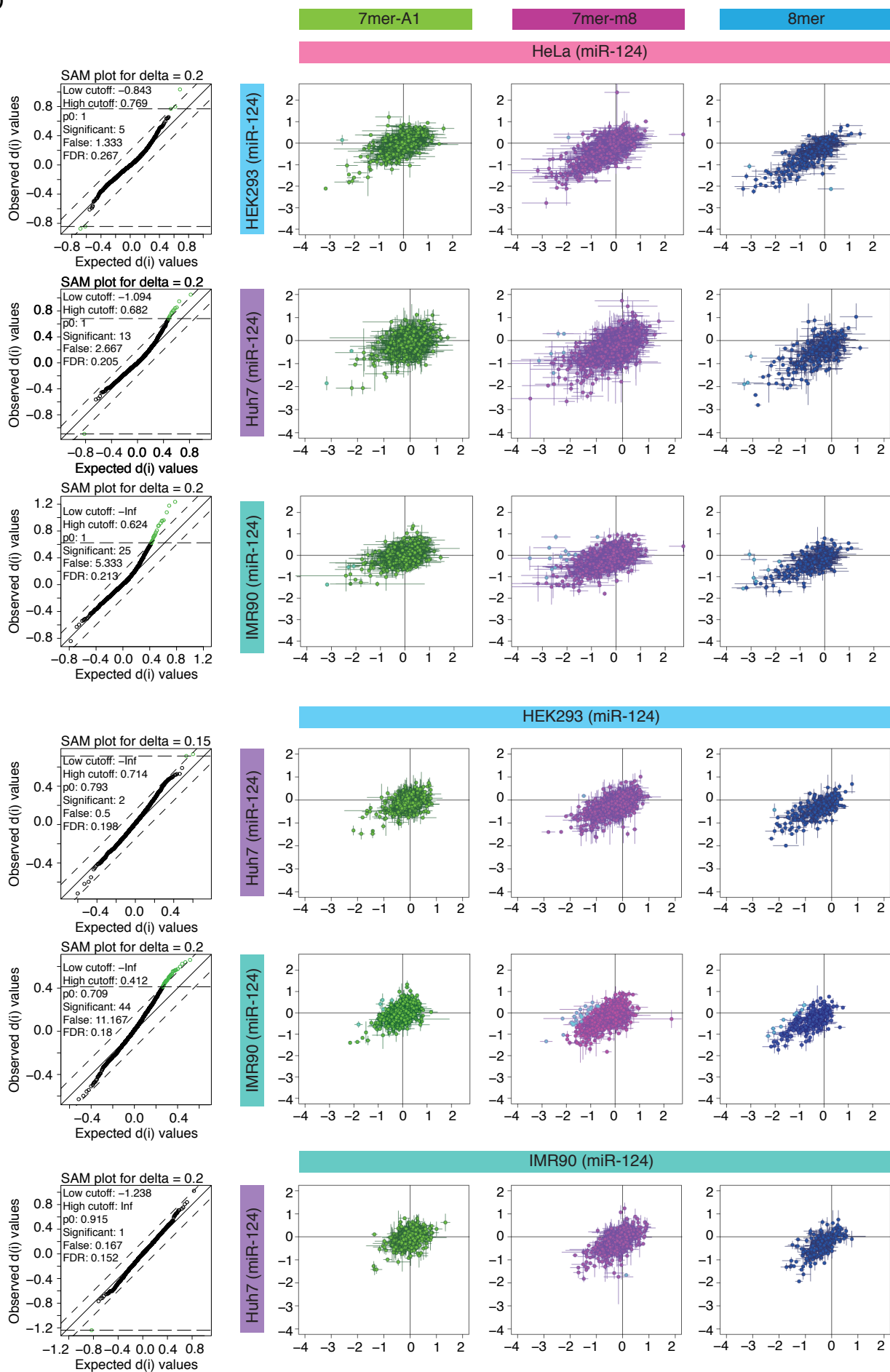
Supplemental Figure 1

C



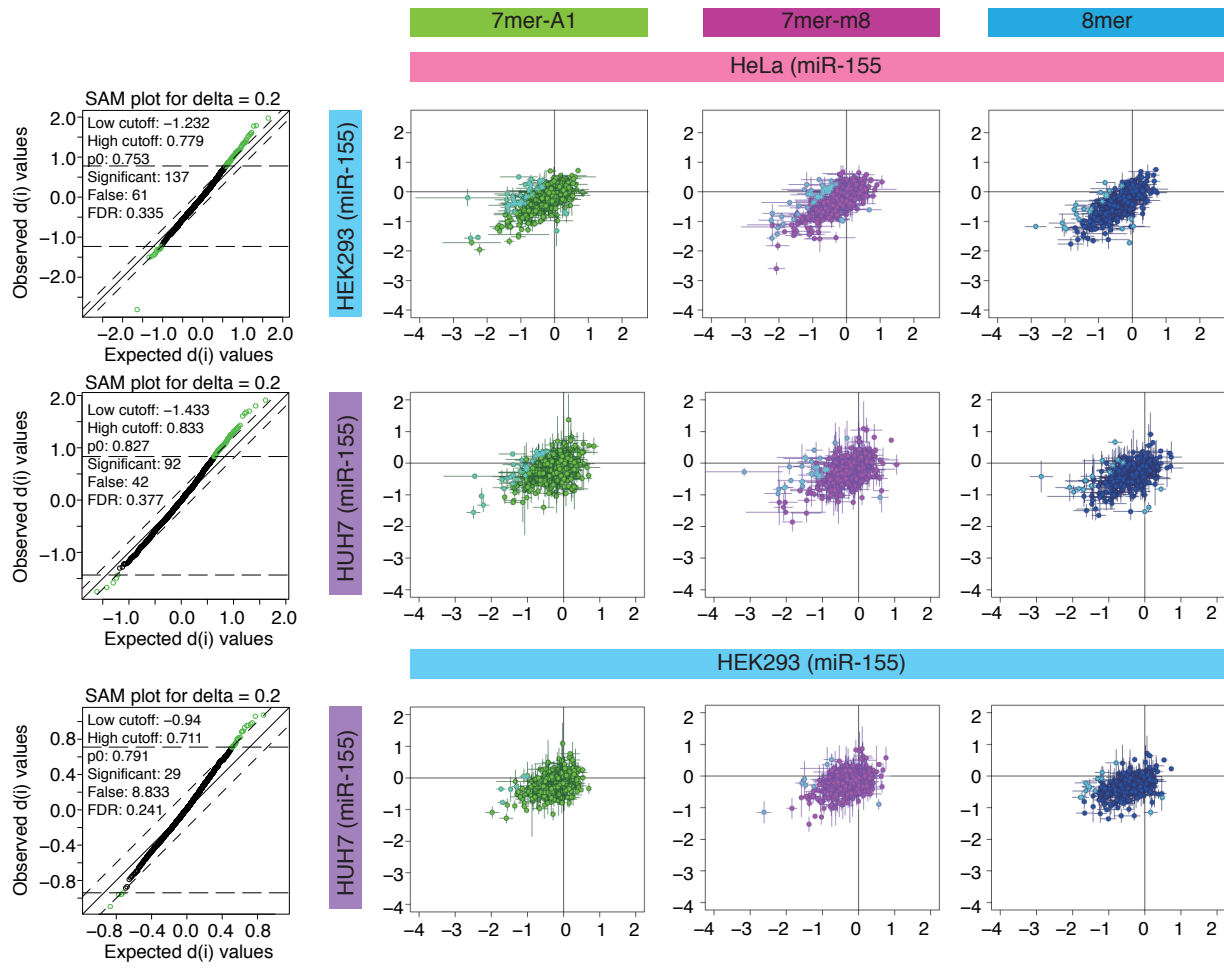
Supplemental Figure 1

D

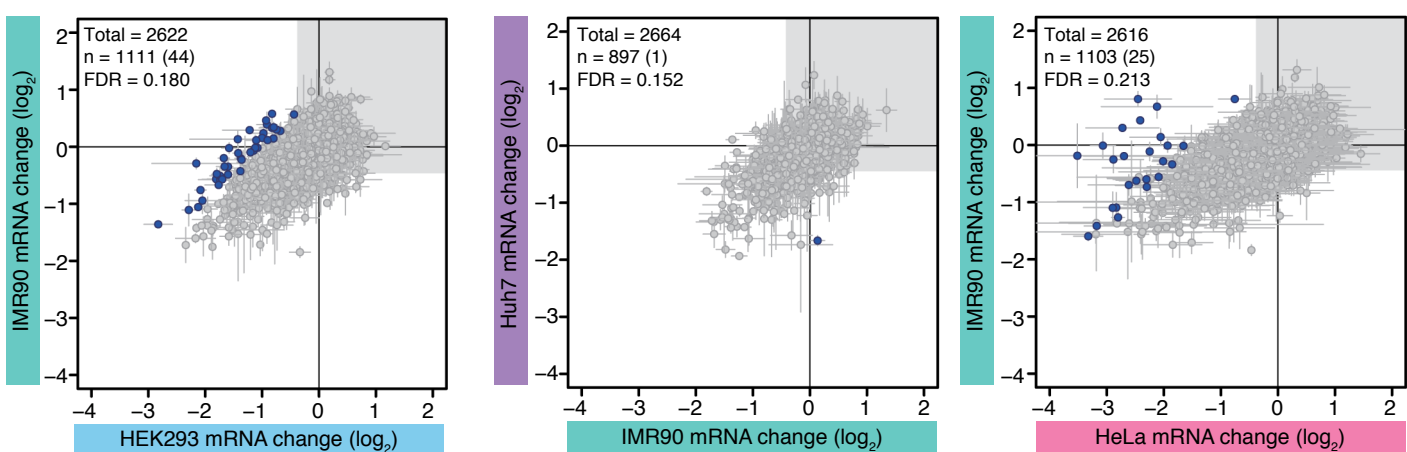


Supplemental Figure 1

D



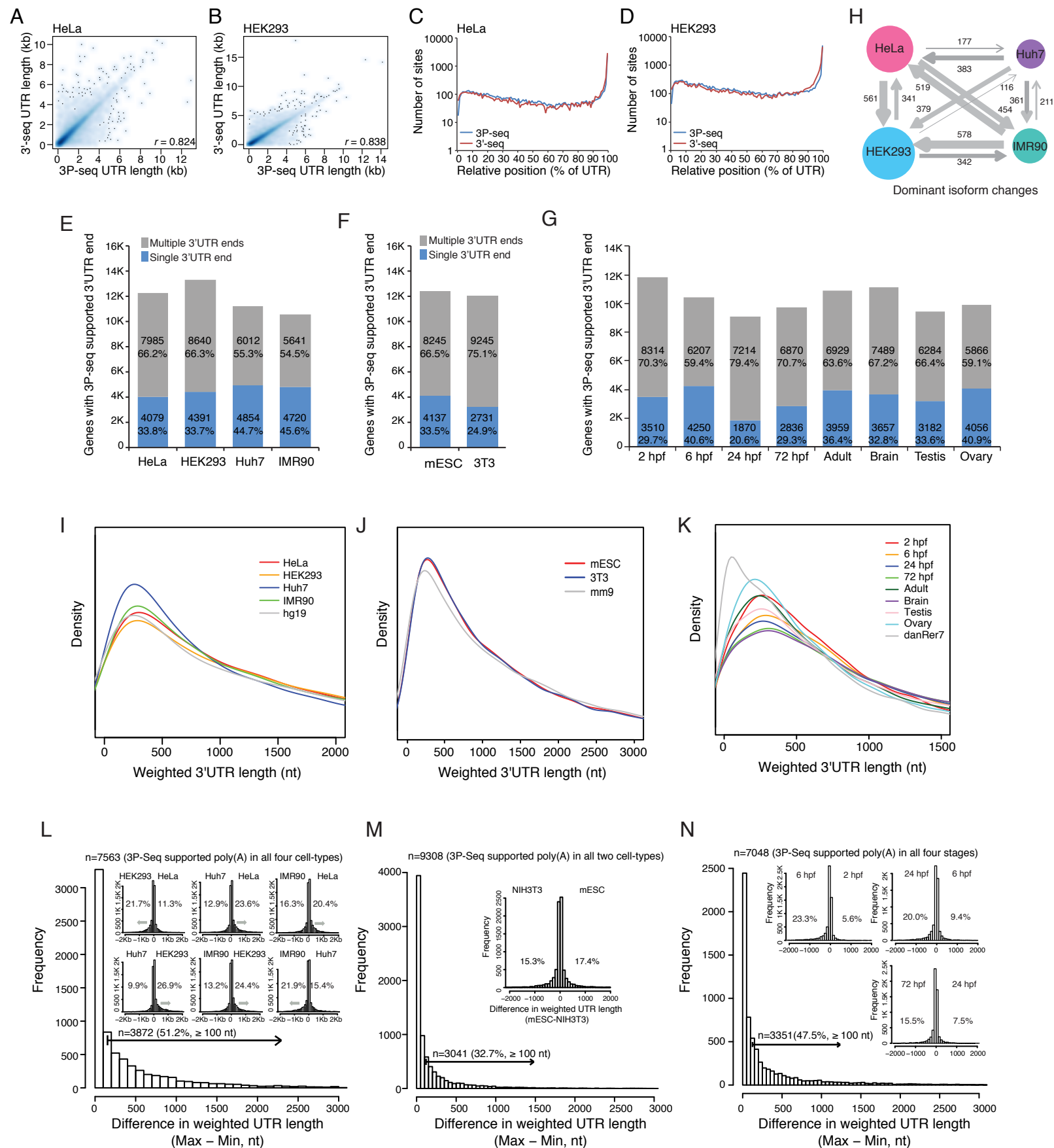
F



Supplemental Figure 1, related to Figure 1. miRNA targeting in different cell lines

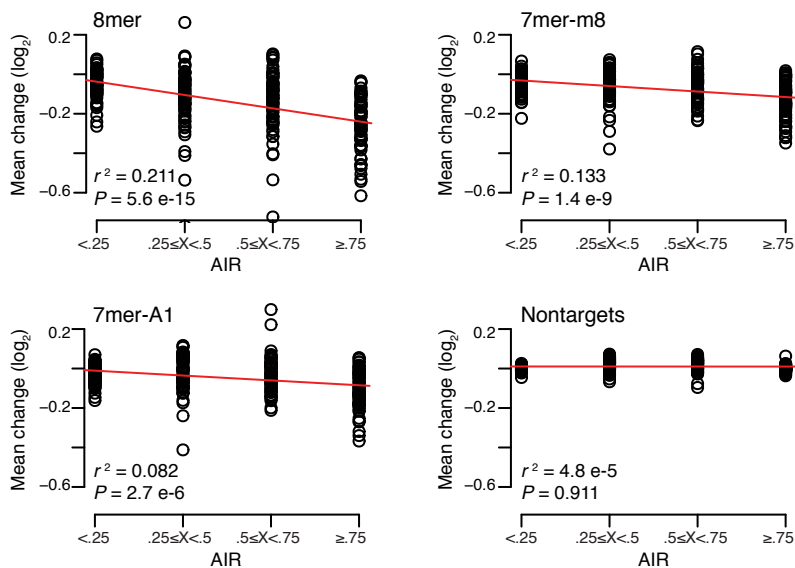
- (A) Repression of predicted miRNA targets following each miRNA transfection. Plotted are cumulative distributions of mRNA changes after transfecting the indicated miRNA (miR-124 or miR-155) into the indicated cell line (HeLa, HEK293, Huh7 or IMR90), considering the sets of mRNAs with the indicated site (8mer, blue; 7mer-m8, green; 7mer-A1, orange; 6mer, purple; no site, black) to the transfected miRNA in their 3'UTR. A difference between the 8mer and no-site distributions is tested (*P* values, Kolmogorov-Smirnov test).
- (B) Enrichment of target sites among the repressed mRNAs. Sylamer analysis (van Dongen et al., 2008) was performed on the transfection datasets shown in (A), after averaging the results of replicates.
- (C) Summary of the procedure used to identify predicted targets that were differentially repressed.
- (D) Analysis of differential repression. For each transfected miRNA, predicted targets were subdivided based on miRNA site type. Predicted targets passing the differential repression threshold are highlighted (green points in significance analysis of microarray (SAM) plots, light blue points in scatter plots).
- (E) Variability of mRNA changes between replicates. Shown are standard deviations of mRNA \log_2 changes in the transfections indicated. Line, median; box, quartiles; whiskers, 1.5 IQR (interquartile range).
- (F) mRNA changes observed after transfecting miR-124 into IMR90 cells compared to those observed after transfecting miR-124 into the other three cell lines (HeLa, HEK293 and Huh7). Otherwise, as in Figure 1A.

Supplemental Figure 2

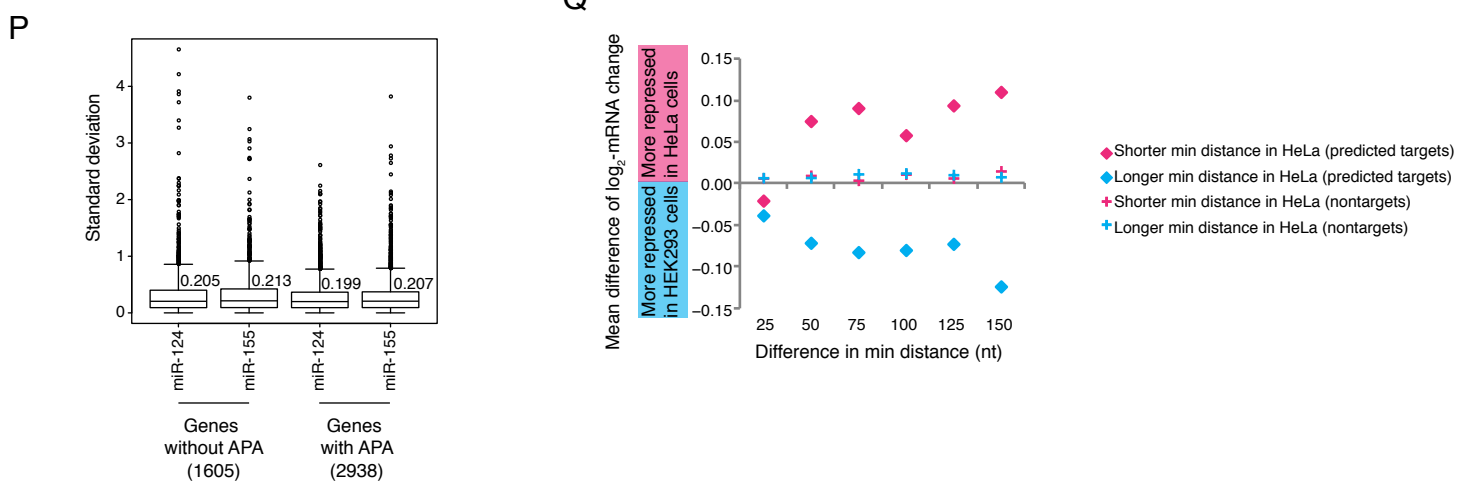


Supplemental Figure 2

O



Q



Supplemental Figure 2, related to Figure 2. Poly(A) site usage in mammalian cell lines and zebrafish samples and its effect on miRNA targeting.

(A, B) Comparison of poly(A) site usage determined by 3P-seq with that determined by 3'-seq (Lianoglou et al., 2013) for HeLa (A) and HEK293 cells (B), the two cell types for which both methods have been applied. For each gene with >10 tags from each method,

the weighted 3'UTR length (a value sensitive to the relative amount of each 3'UTR isoform) was determined using the results from each method and then compared.

(C, D) Comparison of poly(A) sites determined by 3P-seq and 3'-seq. For each gene with >10 tags from each method, the poly(A) site position (relative to entire length of the longest isoform) was determined using 3P-seq (blue) and 3'-seq (red) datasets from HeLa (C) and HEK293 (D) cells.

(E–G) The fraction of genes with multiple and single poly(A) sites, as determined by 3P-seq, for four human cell lines (E), two mouse lines (F), and different zebrafish developmental stages and tissues (G) (Ulitsky et al., 2012).

(H) The number of genes for which the dominant 3'UTR isoform changes between two cell types. The direction of the arrows represents the cell line with the longer isoform, and the width is proportional to the number of genes changing.

(I–K) The weighted lengths of 3'UTRs annotated using 3P-seq data from the four human cell lines (I), the two mouse lines (J), and the eight zebrafish stages and tissues (K) compared to the 3'UTR lengths annotated in the respective reference genomes (hg19, mm9 and danRer7).

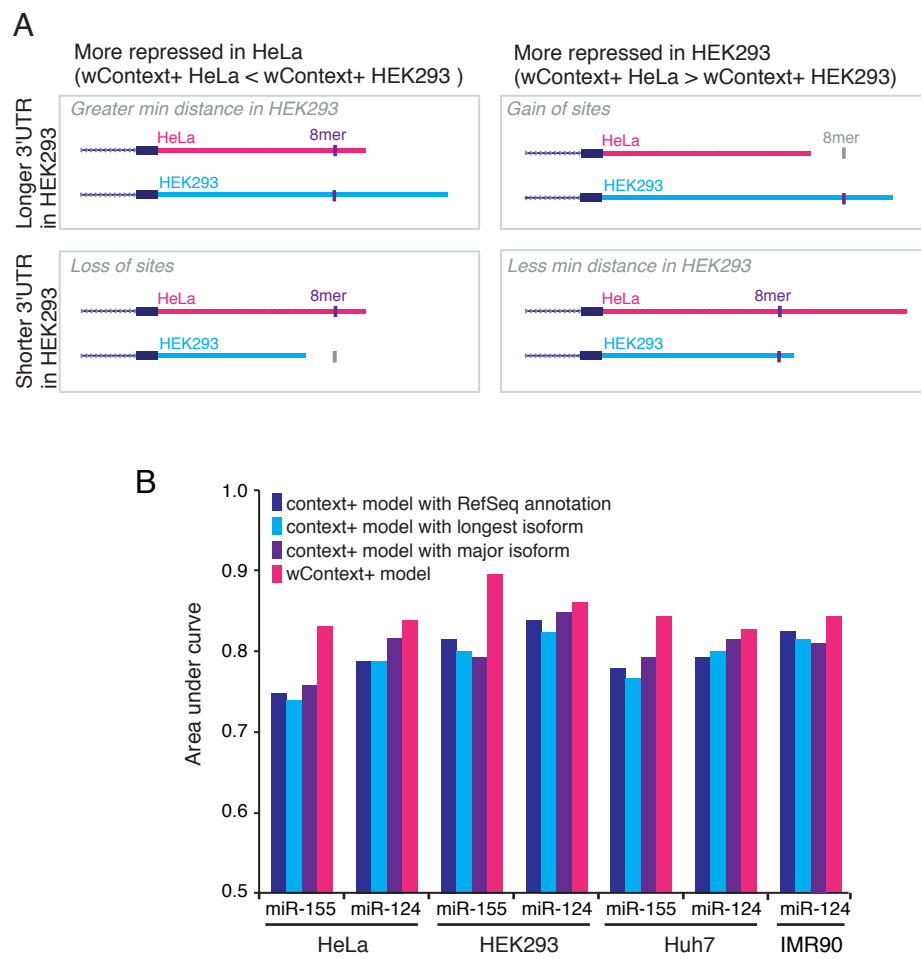
(L–N) Differential use of alternative poly(A) sites in different cellular contexts. Plotted is a histogram of the difference between the longest and shortest weighted 3'UTR lengths

for different cells/stages from each of the three species. Inset: histograms for each pairwise comparison, with percentages indicating the fraction of genes with weighted lengths differing by more than 100 nt.

(O) Relationship between AIR and miRNA-mediated repression. As in Figure 2D–G, but analyzing 74 array datasets.

(P) Variability in expression changes for genes with and without APA. Shown are standard deviations of \log_2 -changes following either miR-124 or miR-155 transfection for genes with and without APA, combining data across the four different cell lines (HeLa, HEK293, Huh7 and IMR90). mRNAs with APA were those that had a weighted 3'UTR changing >100 nt between cell types; genes without APA were those with weighted 3'UTRs changing <10 nt. Median values are shown above the box for each set of genes. Line, median; box, quartiles; whiskers, 1.5 IQR.

(Q) Relationship between changes in minimum distance and miRNA targeting efficacy. Plotted is the difference in repression observed between HeLa and HEK293 cells as a function of the difference in minimum distance observed between these cells (those with a shorter minimum distance in HeLa cells are in pink; in HEK293 cells, blue) for predicted targets (diamonds) and mRNAs that match control sites (nontargets, plus symbols).

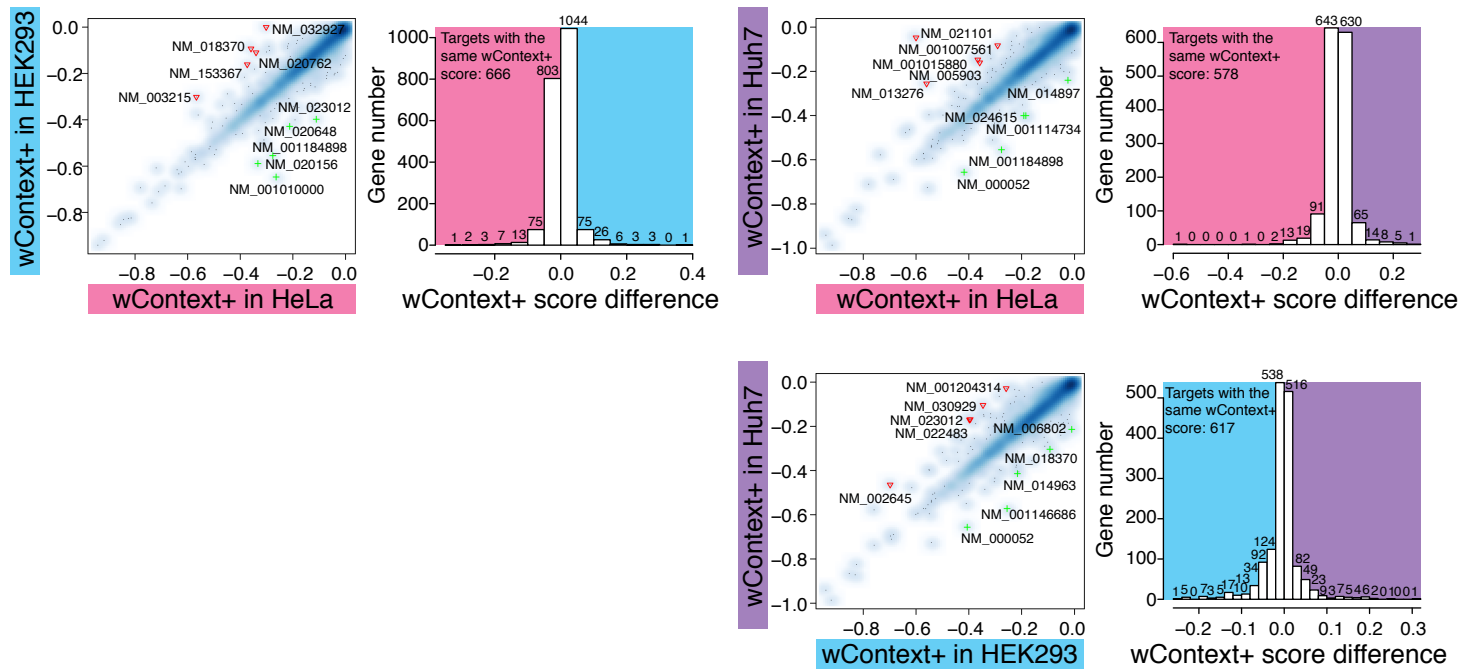


Supplemental Figure 3, related to Figure 3. Performance of the wContext+ model compared to the Context+ model

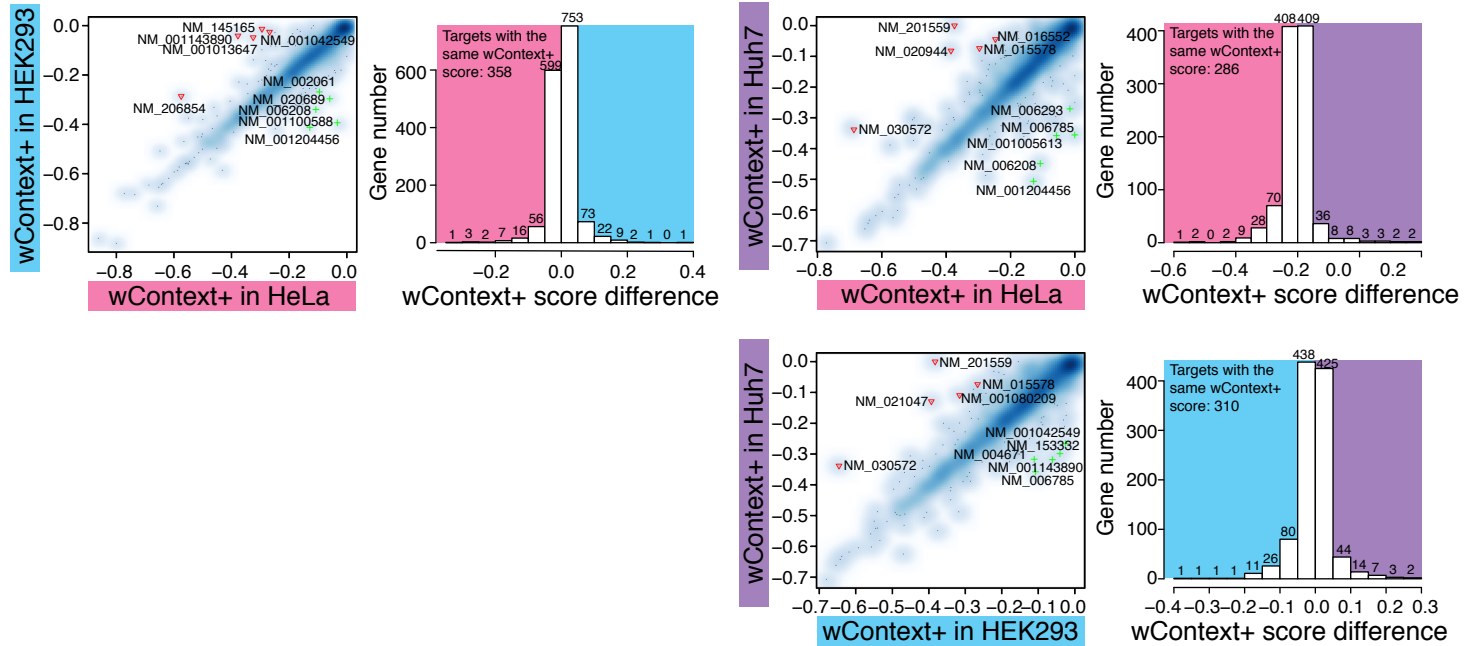
- (A) Overview of how alternative polyadenylation can affect site inclusion or efficacy.
- (B) Performance of target prediction algorithms evaluated by the area under the curve in ROC plots. Otherwise, as in Figure 3B.

Supplemental Figure 4

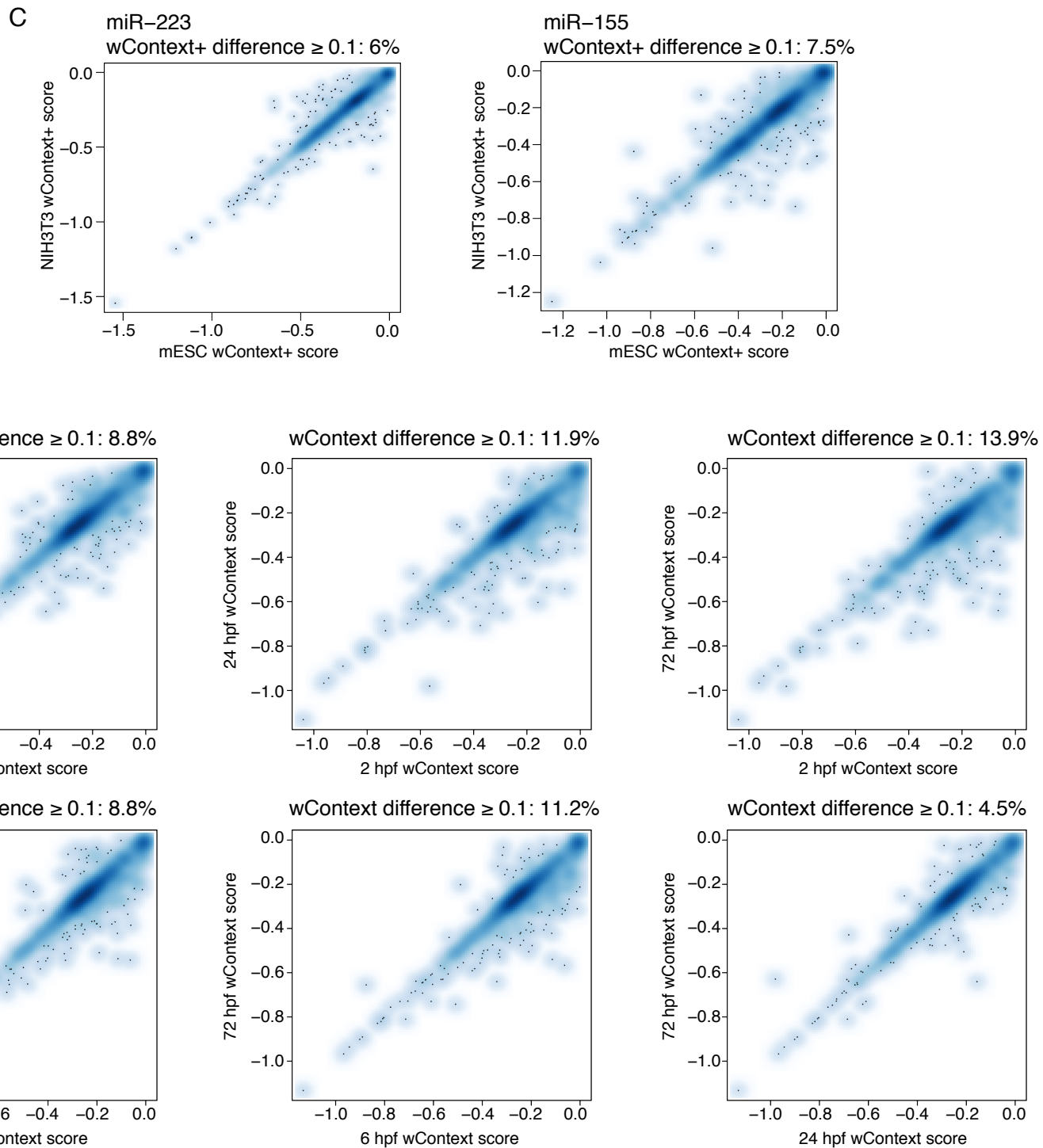
A miR-124 predicted targets



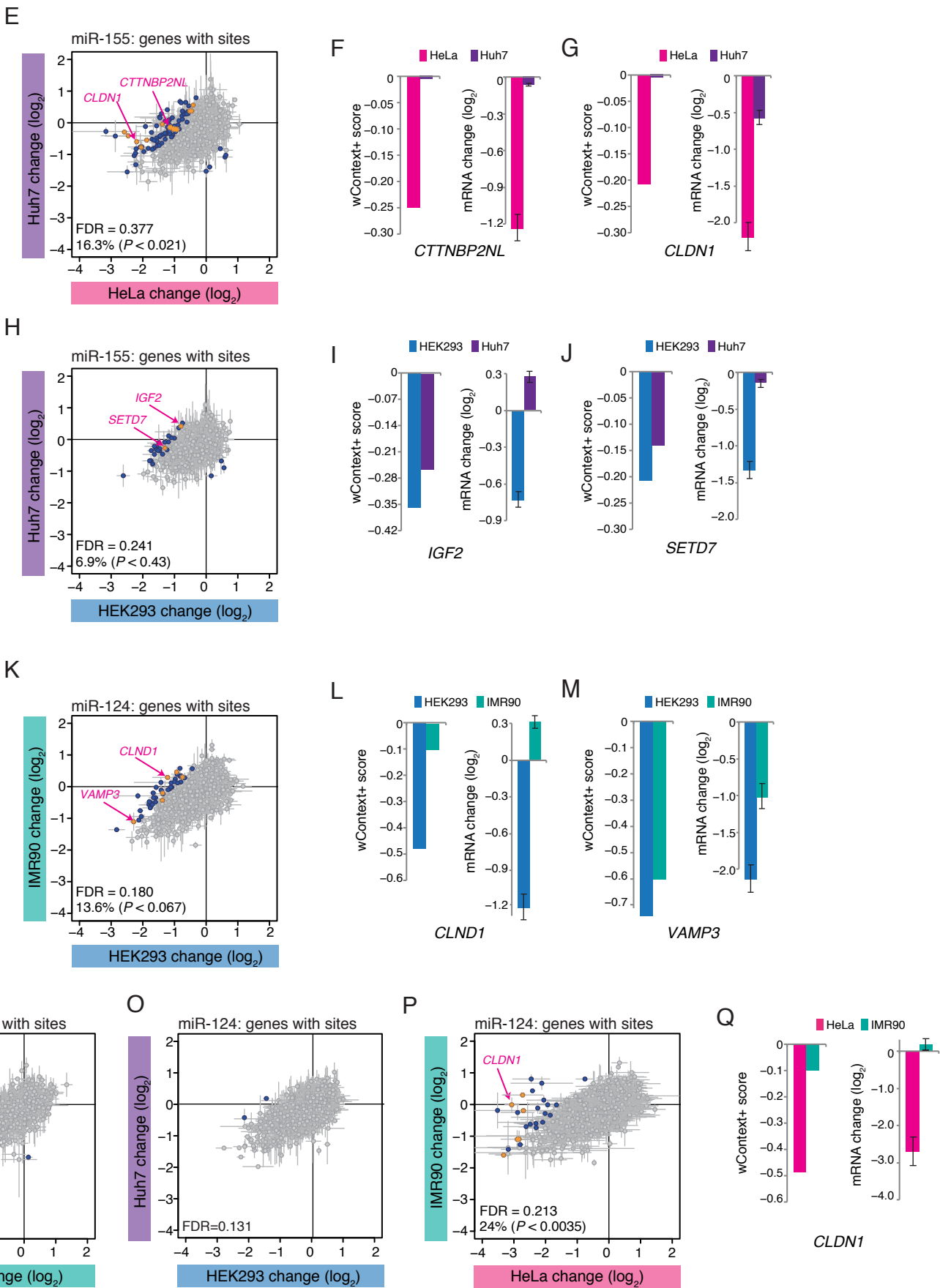
B miR-155 predicted targets



Supplemental Figure 4



Supplemental Figure 4



Supplemental Figure 4, related to Figure 4. The effect of cell type upon the wContext+ score

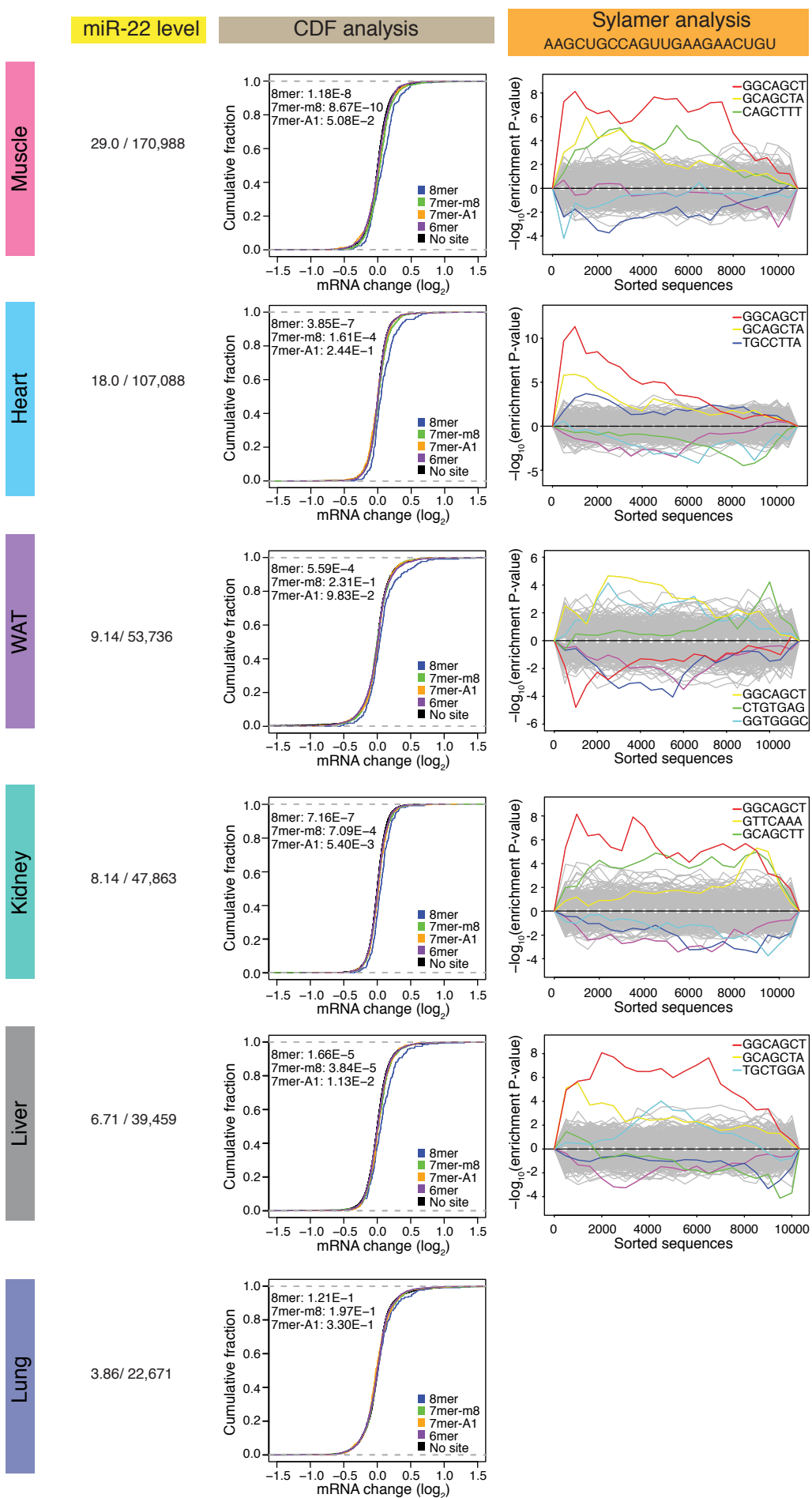
(A, B) Pair-wise comparisons of wContext+ scores of predicted miR-124 (A) and miR-155 (B) targets for the three human cell lines (HeLa, HEK293, and Huh7).

(C, D) Pair-wise comparisons of wContext+ scores for predicted miRNA targets of miR-223 or miR-155 in mouse (C), or miR-430 in zebrafish (D).

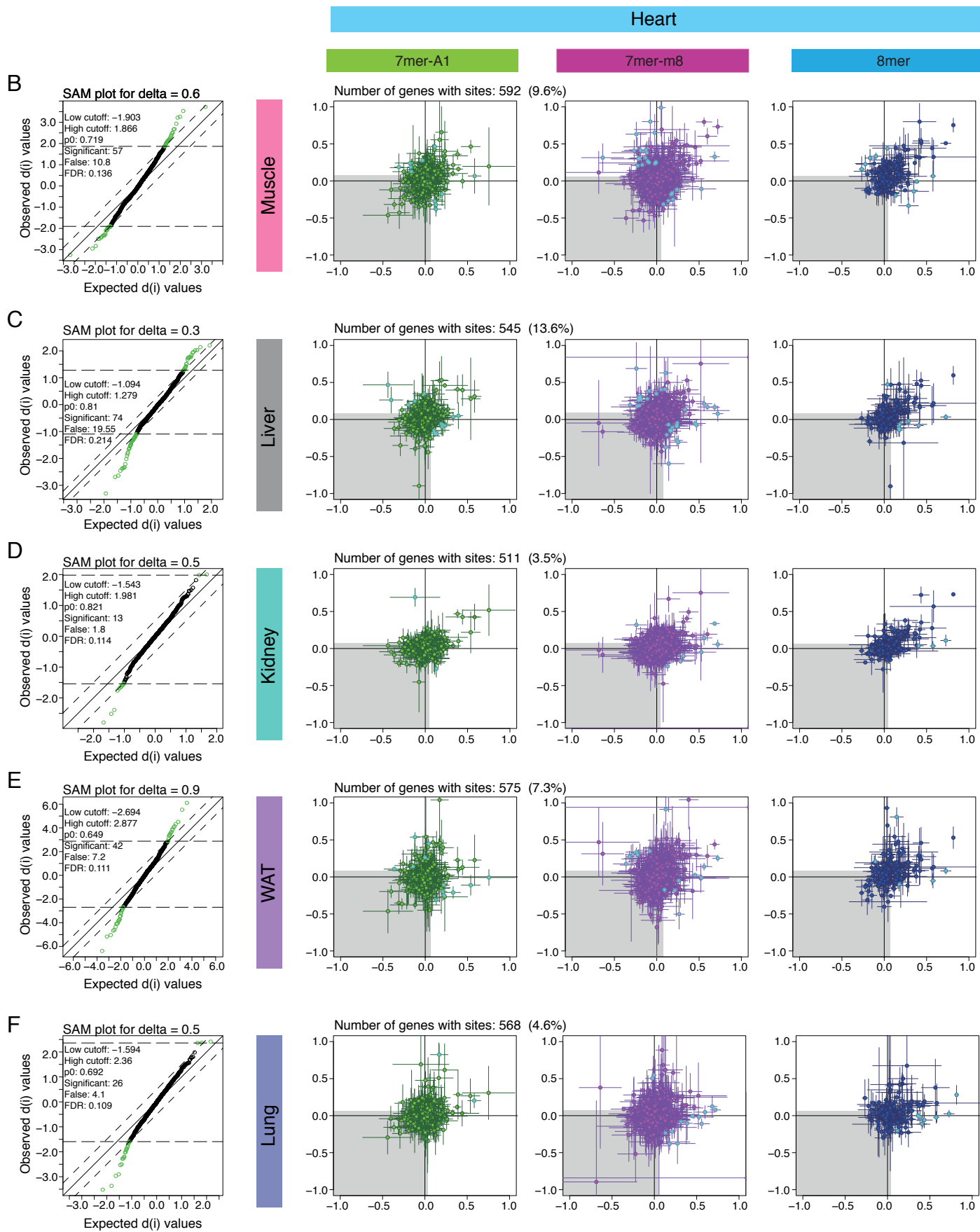
(E–Q) Additional comparisons and examples resembling those of Figure 4. Dots in yellow highlight genes with both significantly different repression and corresponding wContext+ scores that differ by ≥ 0.02 (E), or ≥ 0.03 (H, K, N, O, P).

Supplemental Figure 5

A

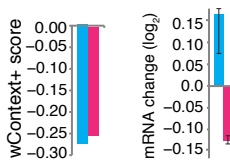
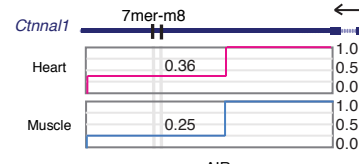
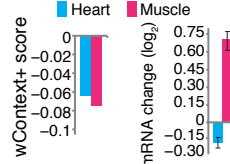
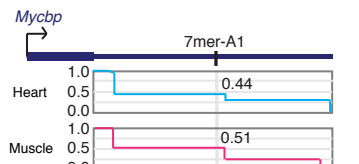
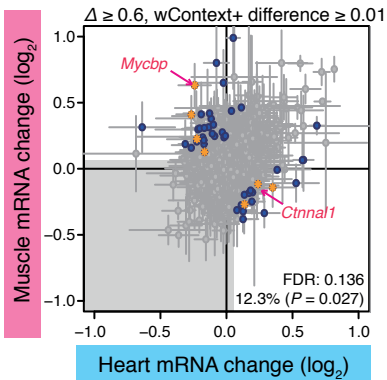


Supplemental Figure 5

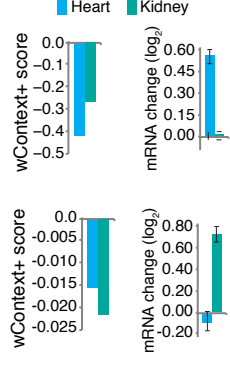
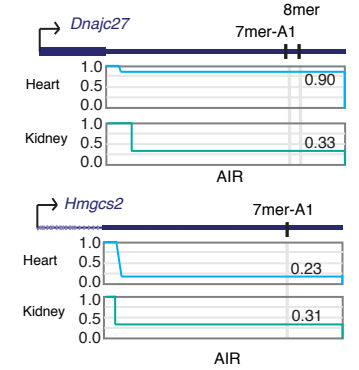
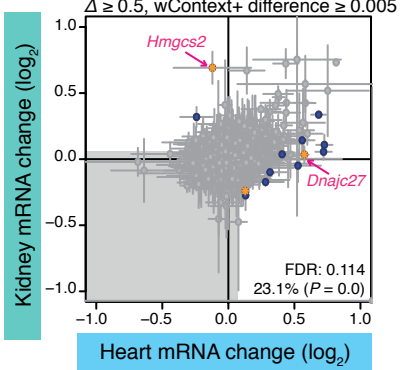


Supplemental Figure 5

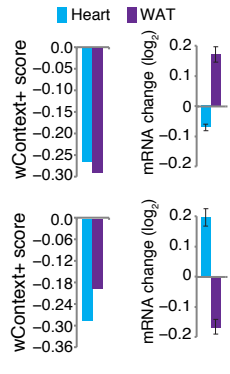
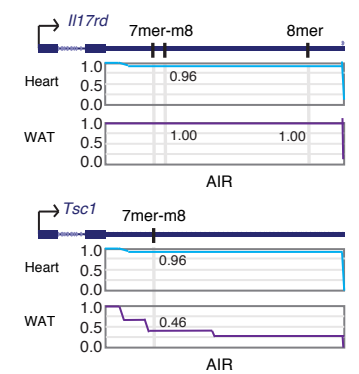
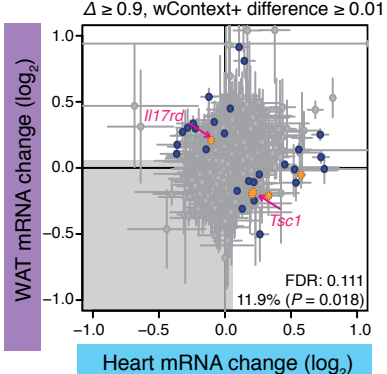
G



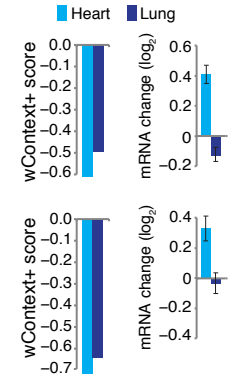
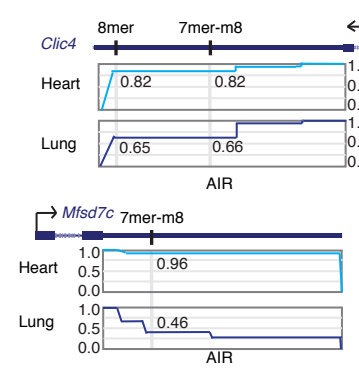
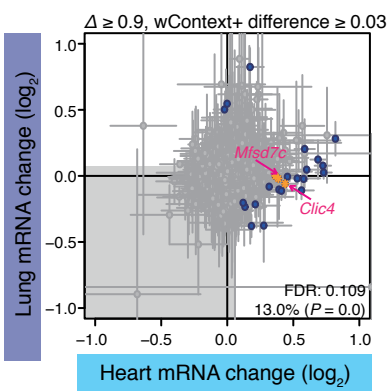
H



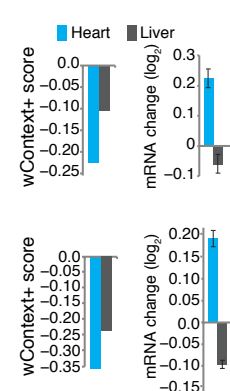
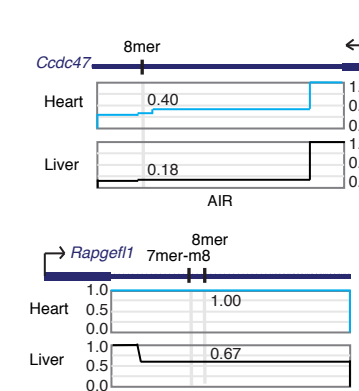
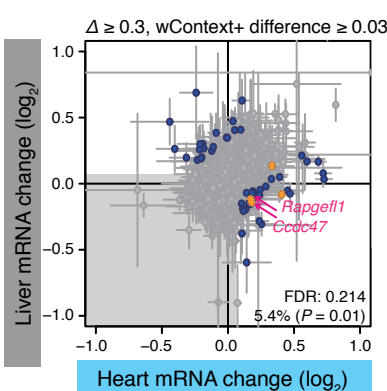
I



J



K



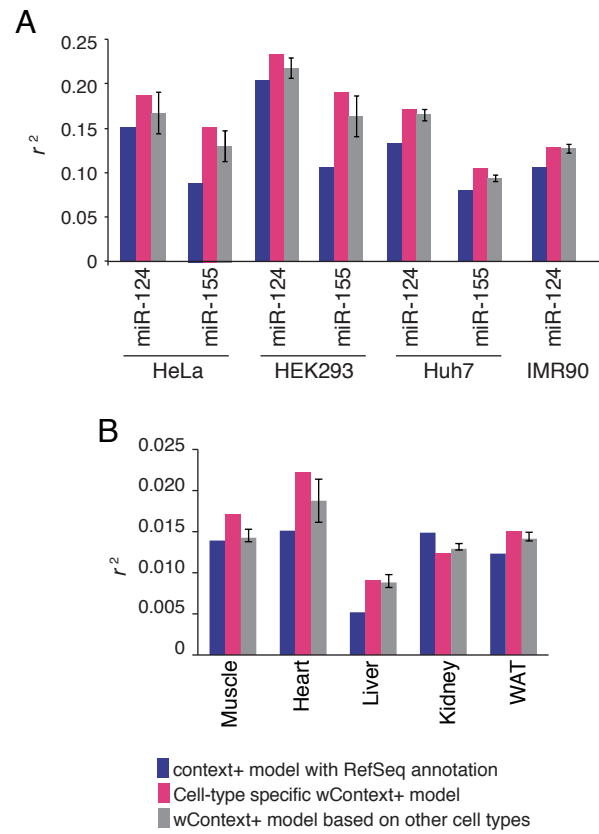
Supplemental Figure 5, related to Figure 5. The differential effects of endogenous miRNAs

(A) Derepression of miR-22 predicted targets in mice lacking miR-22. For each tissue, the repression mediated by miR-22 was observed by comparing mRNA array results from wild-type mice and those lacking miR-22. Otherwise, as in Figure S1A–B. The level of miR-22 are relative values, calculated based on levels of miR-22 measured by RT-PCR and the miR-22 reads in testes, as measured by sRNA-seq in testes (Chiang et al., 2010).

(B–F) miR-22–mediated repression in heart compared to that in the other five tissues profiled (muscle, liver, kidney, WAT and lung). Otherwise, as in Figure S1D.

(G–K) Differential derepression of miR-22 predicted targets. Analyses resemble those of Figures 1 and 4, and blue dots represent targets displaying differential repression, points highlighted in yellow represent targets that are differentially repressed and having different wContext+ scores, and the region corresponding to a \log_2 change < 0.1 is shaded in grey.

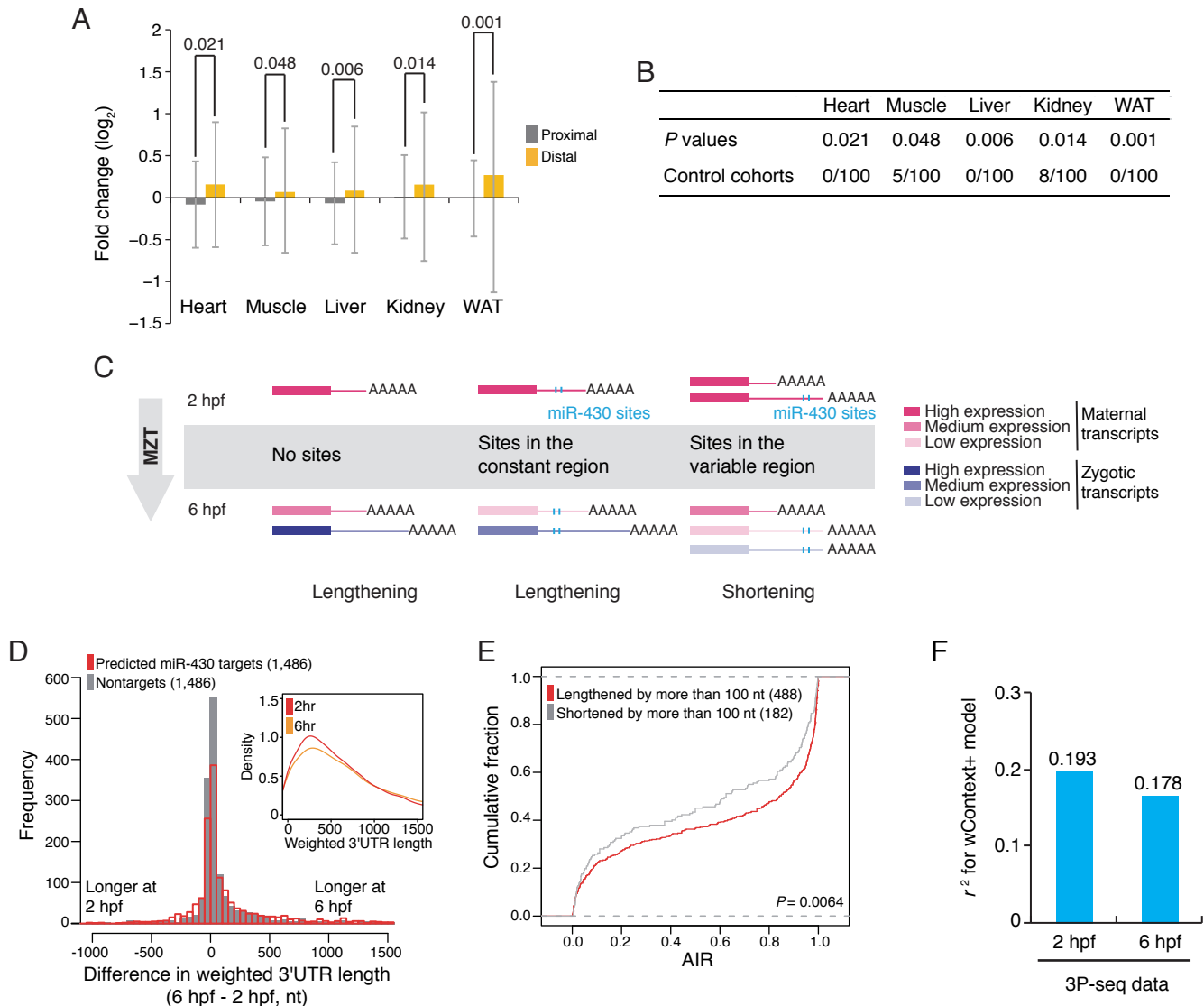
Supplemental Figure 6



Supplemental Figure 6, related to Figure 6. Cell-type–specific wContext+ models outperform non-cell-type–specific models even after excluding genes confidently identified as differentially regulated.

Performance of the indicated models in predicting the effects of exogenous (A) and endogenous miRNAs (B) after excluding targets confidently identified as differentially regulated. Otherwise, as in Figure 6.

Supplemental Figure 7



Supplemental Figure 7, related to Figure 7. miRNA targeting shapes the 3'UTR landscape.

(A) The influence of endogenous miR-22 targeting on differential 3'UTR isoform accumulation. For genes with >10 3P tags and a miR-22 site in their 3'UTR variable regions (AIR between 0.1 and 0.9), the 3P tags were used to quantify accumulation of the isoforms and determine the extent to which accumulation of the distal isoform changed in the *miR-22Δ* compared to wild-type tissues (orange). For comparison, mean changes in proximal isoforms, which lacked miR-22 sites, are also plotted (grey). Error bars, standard error; *P* values (above each pair of bars), paired t-test.

(B) Additional test of the differences observed in (A). *P* values from the t-test are listed, together with the fraction of times that 100 control gene cohorts gave results for which the mean changes of proximal and distal isoforms varied more significantly than observed for the miR-22 predicted targets. For each cohort, the analysis was repeated using genes with a control site, rather than a site to miR-22, in their 3'UTR variable regions, using the same criteria as in (A).

(C) Schematic illustrating the joint influence of zygotic transcription and miR-430 on alternative isoform accumulation. During the maternal-zygotic transition (MZT), the 3'UTR landscape is influenced by zygotic transcription, which tends to increase UTR length, and by the action of miR-430, the major embryonic miRNA (Giraldez et al., 2006). The aggregate effect of these processes differs depending on the position of the miR-430 site.

(D) Changes in weighted 3'UTR lengths of predicted miR-430 targets (red) and a control cohort of genes without miR-430 sites (grey) as embryos pass through the MZT. The

control cohort was randomly selected from genes lacking sites (namely, 8mer, 7mer and 6mer sites) to miR-430. The inset shows the distributions of weighted 3'UTR lengths for genes at 2 and 6 hpf.

(E) Higher AIR observed at 2 hpf for predicted miRNA targets whose 3'UTRs shorten during zebrafish MZT. Plotted are the cumulative distributions of the AIRs for predicted miR-430 targets whose 3'UTRs either lengthened (red) or shortened (grey) by more than 100 nucleotides during MZT. Significance was tested by the Kolmogorov-Smirnov test.

For the 783 genes with miR-430 sites in their constant regions ($\text{AIR} \geq 0.95$), we observed increased accumulation of longer UTR isoforms, presumably because zygotic transcription resulted in overall 3'UTR lengthening. In contrast, for the 1,538 genes with sites in the variable region, we observed more of the shorter isoform, presumably because the long maternal and zygotic isoforms are targeted by miR-430, and thus at 6 hpf these mRNAs have shorter 3'UTRs. Those that lengthened had more miR-430 sites in the 3'UTR constant region (i.e. had a higher AIR) those whose 3'UTRs shortened (~38% vs. ~24 % sites had $\text{AIR} \geq 0.95$, $P = 0.0064$).

(F) Comparison of the performance of the wContext+ model based on 3P-seq data from either 2- or 6-hpf embryos. Values are for predicted targets of miR-430, evaluated using data from Giraldez et al. (2006).

SUPPLEMENTAL TABLES

Supplemental Table 1, related to Figure 1. Differential targeting after transfecting miRNAs into human cell lines.

Cell line 1	Cell line 2	miR-124			miR-155				
		Targets	SDT	SDT _{FDR}	Fraction	Targets	SDT	SDT _{FDR}	Fraction
HeLa	HEK293	1169	4	2.9	0.3%	991	137	91.1	9.2%
HeLa	Huh7	1098	13	10.4	0.9%	921	92	57.3	6.2%
HeLa	IMR90	1103	25	19.7	1.8%	N/A	N/A	N/A	N/A
HEK293	Huh7	1164	2	1.7	0.1%	1013	29	22.0	2.2%
HEK293	IMR90	1111	44	36.1	3.2%	N/A	N/A	N/A	N/A
Huh7	IMR90	897	1	0.9	0.1%	N/A	N/A	N/A	N/A
Average		1090	14.8	11.9	1.1%	975	86.0	56.8	5.9%

Targets, predicted targets with \log_2 changes < -0.3 in either sample

SDT, significantly differential targets

SDT_{FDR}, SDT adjusted by the FDR

Fraction, SDT_{FDR}/Targets

Supplemental Table 2, related to Figure 2. Mapping statistics for 3P-seq libraries.

A. Uniquely mapped 3P tags for the human cell lines.

Sample	Tags
HeLa	5536210
HEK293	4375957
Huh7	4707886
IMR90	3340695
Total	17960748

B. Statistics of 3P clusters and tags.

Sample	Clusters in 3'UTR or downstream regions	Other clusters	Fraction	Cluster tags in 3'UTR or downstream regions	Other cluster tags	Fraction
HeLa	35393	14430	0.71	3623308	525821	0.87
HEK293	42861	19565	0.69	2923958	380549	0.88
Huh7	30587	13708	0.69	1786085	1035002	0.63
IMR90	22421	6504	0.78	2470059	151337	0.94

C. The difference between major 3'UTR isoforms annotated using 3P-seq data in human cell lines and their RefSeq annotations.

Sample	Longer	Shorter	No change	Longer	Shorter	No change
HeLa	1073	2980	5721	11.0%	30.5%	58.5%
HEK293	890	3033	5680	9.3%	31.6%	59.1%
Huh7	743	2679	4785	9.1%	32.6%	58.3%
IMR90	477	2096	4366	6.9%	30.2%	62.9%

D. Uniquely mapped 3P tags for mESCs and NIH3T3 cells.

Sample	Tags
mESC	4743687
NIH3T3	5751050
Total	10494737

E. Statistics of 3P-seq clusters and tags for mESCs and NIH3T3 cells.

Sample	Clusters in 3'UTR or downstream regions	Other clusters	Fraction	Cluster tags in 3'UTR or downstream regions	Other cluster tags	Fraction
mESC	40993	44447	0.48	3207024	465646	0.87
3T3	21156	25445	0.45	3859342	734798	0.84

F. The difference between major 3'UTR isoforms annotated using 3P-seq data in mouse cell lines and their RefSeq annotations.

Sample	Longer	Shorter	No change	Longer	Shorter	No change
mESC	1754	3378	7224	14.2%	27.3%	58.5%
3T3	1452	3041	6483	13.2%	27.7%	59.1%

G. Uniquely mapped 3P tags for the zebrafish samples.

Sample	Uniquely mapped tags
2 hpf	4743687
6 hpf	5751050
24 hpf	7423123
72 hpf	9813474
Adult	7470432
Brain	7905265
Ovary	9233031
Testis	7621156
Total	59961218

H. Statistics of 3P clusters and tags for the zebrafish samples.

Sample	Clusters in 3'UTR or downstream regions	Other clusters	Fraction	Cluster tags in 3'UTR or downstream regions	Other cluster tags	Fraction
2hpf	63719	54762	0.54	3661416	1832790	0.67
6hpf	40595	53755	0.43	3499240	1551141	0.69
24hpf	23268	28626	0.45	4108748	1699501	0.71
72hpf	27090	41024	0.40	5155659	2379962	0.68
Adult	33267	38779	0.46	3804244	1907906	0.67
Brain	25057	42613	0.37	3144426	3705035	0.46
Ovary	32024	36822	0.47	4919208	2257576	0.69
Testis	35304	92435	0.28	3673964	2392767	0.61

I. The difference between major 3'UTR isoforms annotated using 3P-seq data and the zebrafish annotations.

Sample	Longer	Shorter	No change	Longer	Shorter	No change
2 hpf	1605	966	4427	22.9%	13.8%	63.3%
6 hpf	1894	693	4392	27.1%	9.9%	62.9%
24 hpf	2446	791	4620	31.1%	10.1%	58.8%
72 hpf	3107	766	5097	34.6%	8.5%	56.8%
Adult	2138	1279	5011	25.4%	15.2%	59.5%
Brain	2724	523	4780	33.9%	6.5%	59.5%
Ovary	1508	1260	4359	21.2%	17.7%	61.2%
Testis	2860	1125	5495	30.2%	11.9%	58.0%

Supplemental Table 4, related to Figure 5. Uniquely mapping 3P tags from mouse tissues.

Sample	Tags
Heart (KO)	4713978
Heart (WT)	4549578
Muscle (KO)	3181063
Muscle (WT)	5534321
Liver (KO)	4314908
Liver (WT)	5519789
Kidney (KO)	3812740
Kidney (WT)	4892026
Lung (KO)	8669132
Lung (WT)	6916098
WAT (KO)	2710405
WAT (WT)	3734765

SUPPLEMENTAL MATERIALS AND METHODS

Data sources. Human genome assembly hg19, mouse genome assembly mm9, and zebrafish genome assembly danRer7 were used throughout. For annotated mRNA sets, NCBI RefSeq gene annotations (hg19:Aug-22-2011, mm9:Mar-29-2009, and danRer7: Oct-3-2011) were used. Compiled microarray data for 74 mi/siRNA transfections were from(Garcia et al., 2011). Microarray data for miR-223 knockout and wild-type cells were from GEO GSE22003 (Guo et al., 2010), for miR-155 knockout and wild-type cells were from Array Express E-TABM-232 (Rodriguez et al., 2007), and for MZDicer mutant and wild-type zebrafish embryos were from GSE4201 (Giraldez et al., 2006). Denoised 3'-seq datasets for HeLa and HEK293 cells were downloaded from <http://cbio.mskcc.org/leslielab/ApA/atlas> (Lianoglou et al., 2013). The microarray data for miR-22 knockout and wild-type samples are available at the GEO (GSE52940), as are the RNA-seq and 3P-seq datasets (GSE52531).

3P-seq. 3P-seq was as previously published (Jan et al., 2011) but with the following modifications: The splint ligation was done at 18°C overnight instead of at 22°C. After RNase H-mediated release from streptavidin beads, RNA was phenol/chloroform extracted, passed through a P-30 column (Bio-Rad) and ethanol-precipitated. 1 µl of RNase T1 was used instead of 3 µl. For the 3' adapter ligation, the reaction volume was scaled to 8 µl, 12.5% PEG8000 was added, and ethanol precipitation prior to gel purification was omitted. A 3:1 ethanol to water ratio with 1.5 µl glycoblue (Life Technologies) was used for all precipitations. After both gel purifications, rather than eluting overnight, the gel slices were crushed by spinning through a 20-gauge hole in a 0.5 ml tube, frozen for 20 minutes at -80°C in 800 µl 0.3 M NaCl, thawed at 50°C for 20 minutes with occasional vortexing, and rotated at room temperature for 20 minutes. A detailed revised protocol is available online at bartellab.wi.mit.edu/protocols/.

Processing of 3P-seq reads and determining mRNA poly(A) sites. Using Bowtie (Langmead et al., 2009), 88 million reads mapped uniquely to the genome with at least one terminal untemplated adenylate residue. These were carried forward as 3P tags (Table S2A). Tags within 15 nt of the most frequently sequenced tags were clustered together, and these clusters were considered poly(A) sites if they contained at least two identifiably independent tags (i.e. tags with a different number of untemplated terminal adenylates, or from two different libraries).

Poly(A) sites assigned to protein-coding genes mapped to either the longest annotated 3'UTR of a gene or 5000 (mammals) or 3000 (zebrafish) nt downstream of the 3'UTR end, disallowing overlap with the downstream gene (Table S2). This accounted for 28–78% of the poly(A) sites and 46–94% of the 3P tags. Another 6–16% of the poly(A) sites (1–8% percent of tags) mapped to exonic or intronic regions upstream of stop codons, indicating instances of alternative last exons, where were not considered in this study, and 0.1–5% of the poly(A) sites (0.1–3% percent of tags) were assigned to non-coding RNAs (ncRNAs). The remainder might be poly(A) sites for unannotated mRNAs, long non-coding RNAs (Nam and Bartel, 2012; Ulitsky et al., 2012), tags filtered with our criteria, or false positives.

Weighted 3'UTR lengths and weighted minimum distance of sites. For each mRNA, the weighted 3'UTR length was calculated by summing the 3'UTR length of each isoform weighted by the number of 3P tags representing that isoform. Similarly, the weighted minimum distance of a site was calculated by summing the minimum distance of that site weighted by the ratio of corresponding 3'UTR isoforms containing the site.

Processing of RNA-seq reads and measuring expression level. All RNA-seq data were mapped to the human reference genome using Bowtie version 0.12.8 (Trapnell et al., 2009), allowing at most five genomic matches but choosing the best one (-n 1 -e 240 -m 5 --best --strata). To measure expression levels we used reads per kilobase per million reads (RPKM) values, mapping

to RefSeq annotations, and to decide which genes to consider we used reads per million reads (RPM) values. Quantile normalization was performed to reduce technical global bias of expression between replicates and between mock-transfected and transfected cells (Bolstad et al., 2003).

Analysis of miRNA responses. For RNA-seq expression analyses, we considered only those genes with >3 RPM in the mock-transfected samples, which dramatically reduced the variance observed between replicates. Likewise, for analysis of the precompiled 74 microarray datasets, we considered only those genes with >10 RPM (as measured by RNA-seq from HeLa samples). For analysis of mouse and zebrafish microarray data, we considered only the genes expressed above the median level in the absence of the miRNA.

Context score models. The context scores and total context scores were calculated as described (Garcia et al., 2011), except the upper bound for the score of each site depended on its type, with 8mer, 7mer-m8, and 7mer-A1 sites having an upper-bounds of -0.03, -0.02, and -0.01, respectively. Species-specific TA values were estimated as described (Garcia et al., 2011). For wContext+ scores, a weighted minimum distance was calculated using corresponding 3P-seq data. For each site, the wContext+ score was calculated by weighting its context+ score with its AIR. Because the Context+ score represented a log₂-scaled fold change, this calculation was done in natural-value space and the result switched back to log₂-scaled space (Figure 3A). For each target, wContext+ scores for all sites to the miRNA were summed to yield the total wContext+ scores.

Identifying differentially repressed targets. We adapted the Significance Analysis of Microarrays (SAM) approach (Tusher et al., 2001) to identify differentially repressed miRNA targets, using the R ‘siggenes’ package (Schwender, 2012). For each cell line, we computed log₂

fold changes for each gene using the ratio of normalized gene expression values in the miRNA-transfected library vs. the matched mock-transfected RNA-seq library (e.g., GSM1269344 vs. GSM1269348). For each pair of cell types, we implemented the following steps:

- i) To correct for global biases (e.g., those derived from variable transfection efficiency), we performed median-based centering of fold changes. We then scaled the fold changes such that the slope of the linear regression function equaled 1 (Figure S1C).
- ii) For each gene i in cell lines A and B, we computed the quantity $d(i) = (\mu_{Ai} - \mu_{Bi}) / (\sigma_i + c)$. Here, μ_{Ai} is the mean of all \log_2 fold changes for gene i in cell type A; σ_i is the pooled standard deviation of all \log_2 fold changes for gene i in cell lines A and B, and c is a constant used to minimize the coefficient of variation (Tusher et al, 2001). We permuted the \log_2 fold changes to estimate an expected $d(i)$ value for each gene. A delta (Δ) value was calculated by subtracting the expected $d(i)$ from the observed $d(i)$.
- iii) We considered genes to be significantly differently affected if they surpassed a Δ threshold of 0.2. An FDR was calculated as the median number of genes that surpassed this threshold when using the permutations. When analyzing expression changes following miRNA transfection, genes with APA and those without displayed similar variability (Figure S2P).

Plasmid construction. To generate luciferase reporters, ~500–800 nt 3'UTR fragments from differentially repressed predicted targets were amplified from genomic DNA using nested PCR. These amplicons were digested at the specified sites and ligated into digested pIS1 (Grimson, et al., 2007). The miR-155 site(s) were then mutated with the indicated oligonucleotides using the QuikChange mutagenesis kit or QuikChangeMulti mutagenesis kit (Agilent). Plasmids are deposited in Addgene.

HK1. Primers for the first PCR: GCGAGAACAGAGGACTGGAC and GATGCACG CCTGTAGTCTCA. Primers for the second PCR: CTAGTCTAGAGAGTCCGGATCCCCAG

CCTACTG (containing XbaI site) and GCGCACTAGCGGCCGCGACACGGCTCACAAAGC GGTGGG (containing NotI site). Mutation oligonucleotides: CTGAAGGCGAGTGTGGGCATA aCgTaAGCTGCTTCCTCCCCTCCTG and CAGGAGGGAGGAAGCAGCTtAcGtTATGCC ACACCTCGCCTTCAG.

ATP2B2. Primers for the first PCR: TGTTAGGGCCCAGATTAC and GAGGACAG TGGGTTGGAGAG. Primers for the second PCR: CTAGTCTAGAGGGTGGACTATCTT GAAGAACCC (containing XbaI site) and GCGCACTAGCGGCCGCTGACATCTGTTATG AAAATTACC (containing NotI site). Mutation oligonucleotides: CTGTAATTCTACCAGA AATTCCAGAaCgTaATGTAGGTAGAAAAAAATGCAAGCAAGC and GCTTGCTTGCATTTCTACCATtAcGtTCTGGAAATTCTGGTAGAAATTACAG

PELO. Primers for the first PCR: AGCTGCAAGAATGGCACTTT and GGAATGACTT CCAGCTTG. Primers for the second PCR: CTAGTCTAGACACACTGCATGCTTG AAACAG (containing XbaI site) and GCGCACTAGCGGCCGCGCTCAAGGAGATTA TTTGAC (containing NotI site). Mutation oligonucleotides: GGAAATTCTGGTTGGTT GTTGTGTTaCgTaAGTCATATTGATTAGAGGGTAACCTAAATC and GATTAAAG TTACCCCTCAAATCAAATGACTtAcGtTAACAACAACAAACCAAGAATT CC.

INSIG2. Primers for the first PCR: ATTGCCAGGATGCAGTTTC and ATCTGCC TTGTGGATCAG. Primers for the second PCR: CTAGTCTAGAGTATTCTCTTTAGC TTACTG (containing XbaI site) and GCGCACTAGCGGCCGACAGAACCCAATAG AAGACAGAACCC (containing NotI site). GTATATGTGATGAGCAGAAGAGGTTATCA aCgTcAAATTGTTGGTTCAAATTGGAACAG and CTGTTCAAATTAGAA CAAAACAATTgAcGtTGATAACCTCTGCTCATCACATATAC.

EPAS1. Primers for the first PCR: GGTATAGTGACCCGTCCAC and TGGGTTCCCCATAGGATACA. Primers for the second PCR: CTAGTCTAGA CTTTGCAACTCCCTGGGTAAGAG (containing XbaI site) and GCGCACTAGCGGCCGC

GTAAAGCTCCCATAACAGTTATAATGTTG (containing NotI site). Mutation oligonucleotides:
GTAAATCATATTTAGCTGCACGAGTCaACCCCACACAGGGTGGCAG (site 1) and
GATTTCCTGTGTGTTGCCCTGAGTCaAAGGGCATTACCCCTGCAG (site 2)

LPIN1. Primers for the first PCR: GGATGGGCCCTTACAGTAT and TAGTGAACA
AGCGCAGAGGA. Primers for the second PCR: CTAGTCTAGAGACTGACCTCTTTGGA
ATTCTG (containing XbaI site) and GCGCACTAGCGGCCGCTGCAAAAGGAAATCTG
CACATGC (containing NotI site). Mutation oligonucleotides: GGTAAAAGATTTGCTTACT
TTTCGAAaCgTaATTTTTAAAGAGTGTACTCCAACGATTG and CAATCGTTGG
AGTAAAACACTCTTAAAAAAATtAcGtTTCGAAAAGTAAAGCAAAATCTTACC.

ELOVL6. Primers for the first PCR: AAACTGTGCGAGCACACAC and GGCCCTT
TGTTGTCAACTGT. Primers for the second PCR: CTAGTCTAGAGCTGTAGACCC
CATGAGAAAAGATG (containing XbaI site) and GCGCACTAGCGGCCGCGTTAT
GAGTGTGTGAAGTCAAAC (containing NotI site). Mutation oligonucleotides:
GTAATTCTACTCTTAAGTGAGATATGAAaCgTaATCCTTGTTCAGTTGCC and
GGGGCAACTGAACAAAAGGATtAcGtTTCATATCTCACTTAAGAGTAGAAATTAC.

LMBRD2. Primers for the first PCR: TGGGGGATTTTGCATGTAT and
GGTGGGATACTTGAGGGTGA. Primers for the second PCR: CTAGTCTAGA
CTTCAAGTGATGCGTGTCTGTG (containing XbaI site) and GCGCACTAGCGGCCGC
GGTAAAAACAGTCTATTAGTAAG (containing NotI site). Mutation oligonucleotides:
GTTGATTATGATATTCAAGGATAAACCTAGAGTCaAATGAAAAATAGTTTTTTAA
GTAGTCAAAGAG and CTCTTGACTACTAAAAAAACTATTTTCATTtAcGtCT
AGGATTATCCTGAATATCATAATCAAC.

IL6R. Primers for the first PCR: AGAACCATGCTAGCGGAAGA and AAGACCACC
AACTCCACCTG. Primers for the second PCR: CTAGTCTAGAGTGTCTCAATGCACGGGG
CATTTC (containing XbaI site) and GCGCACTAGCGGCCAGCCTGCCACTGG
GCCCTG (containing NotI site). Mutation oligonucleotides: GGCCTAAAGTAAAATGATCA

ATAATGTTGTAaCgTaAATGAAATATTTCAAGAAATGTGTCCAGGGG and
CCCCTGGACACATTCTTGA~~AAA~~ATTCATTtAcGtTACAAACATTATTGATCATTAA
CTTTAGGCC.

SUPPLEMENTAL REFERENCES

- Bolstad, B.M., Irizarry, R.A., Astrand, M., and Speed, T.P. (2003). A comparison of normalization methods for high density oligonucleotide array data based on variance and bias. *Bioinformatics* *19*, 185–193.
- Chiang, H.R., Schoenfeld, L.W., Ruby, J.G., Auyueung, V.C., Spies, N., Baek, D., Johnston, W.K., Russ, C., Luo, S., Babiarz, J.E., et al. (2010). Mammalian microRNAs: experimental evaluation of novel and previously annotated genes. *Genes Dev.* *24*, 992–1009.
- Garcia, D.M., Baek, D., Shin, C., Bell, G.W., Grimson, A., and Bartel, D.P. (2011). Weak seed-pairing stability and high target-site abundance decrease the proficiency of lsy-6 and other microRNAs. *Nat. Struct. Mol. Biol.* *18*, 1139–1146.
- Giraldez, A.J., Mishima, Y., Rihel, J., Grocock, R.J., van Dongen, S., Inoue, K., Enright, A.J., and Schier, A.F. (2006). Zebrafish MiR-430 promotes deadenylation and clearance of maternal mRNAs. *Science* *312*, 75–79.
- Guo, H., Ingolia, N.T., Weissman, J.S., and Bartel, D.P. (2010). Mammalian microRNAs predominantly act to decrease target mRNA levels. *Nature* *466*, 835–840.
- Jan, C.H., Friedman, R.C., Ruby, J.G., and Bartel, D.P. (2011). Formation, regulation and evolution of *Caenorhabditis elegans* 3'UTRs. *Nature* *469*, 97–101.
- Langmead, B., Trapnell, C., Pop, M., and Salzberg, S.L. (2009). Ultrafast and memory-efficient alignment of short DNA sequences to the human genome. *Genome Biol.* *10*, R25.
- Lianoglou, S., Garg, V., Yang, J.L., Leslie, C.S., and Mayr, C. (2013). Ubiquitously transcribed genes use alternative polyadenylation to achieve tissue-specific expression. *Genes Dev.* *27*, 2380–2396.
- Nam, J.-W., and Bartel, D.P. (2012). Long noncoding RNAs in *C. elegans*. *Genome Res.* *22*, 2529–2540.
- Rodriguez, A., Vigorito, E., Clare, S., Warren, M.V., Couttet, P., Soond, D.R., van Dongen, S., Grocock, R.J., Das, P.P., Miska, E.A., et al. (2007). Requirement of bic/microRNA-155 for normal immune function. *Science* *316*, 608–611.
- Schwender, H. (2012). siggenes: Multiple testing using SAM and Efron's empirical Bayes approaches. R package, version 1.36.0.
- Trapnell, C., Pachter, L., and Salzberg, S.L. (2009). TopHat: discovering splice junctions with RNA-Seq. *Bioinformatics* *25*, 1105–1111.
- Tusher, V.G., Tibshirani, R., and Chu, G. (2001). Significance analysis of microarrays applied to the ionizing radiation response. *Proc. Natl. Acad. Sci. U.S.A.* *98*, 5116–5121.
- Ulitsky, I., Shkumatava, A., Jan, C.H., Subtelny, A.O., Koppstein, D., Bell, G.W., Sive, H., and Bartel, D.P. (2012). Extensive alternative polyadenylation during zebrafish development. *Genome Res.* *22*, 2054–2066.

van Dongen, S., Abreu-Goodger, C., and Enright, A.J. (2008). Detecting microRNA binding and siRNA off-target effects from expression data. *Nat Meth* 5, 1023–1025.